[CANCER RESEARCH 64, 5415–5424, August 1, 2004]

Fenretinide Cytotoxicity for Ewing's Sarcoma and Primitive Neuroectodermal Tumor Cell Lines Is Decreased by Hypoxia and Synergistically Enhanced by Ceramide Modulators

Sandeep Batra,[1] C. Patrick Reynolds,[1,2,3,4] and Barry J. Maurer[1,2,3,5]

[1]Division of Hematology-Oncology, Children's Hospital Los Angeles; [2]University of Southern California-Children's Hospital Los Angeles Institute for Pediatric Clinical Research; and Departments of [3]Pediatrics, [4]Pathology, and [5]Cell and Neurobiology, University of Southern California, Keck School of Medicine, Los Angeles, California

ABSTRACT

Patients with disseminated Ewing's family of tumors (ESFT) often experience drug-resistant relapse. We hypothesize that targeting minimal residual disease with the cytotoxic retinoid *N*-(4-hydroxyphenyl) retinamide (4-HPR; fenretinide) may decrease relapse. We determined the following: (*a*) 4-HPR cytotoxicity against 12 ESFT cell lines *in vitro*; (*b*) whether 4-HPR increased ceramide species (saturated and desaturated ceramides); (*c*) whether physiological hypoxia (2% O_2) affected cytotoxicity, mitochondrial membrane potential ($\Delta\Psi_m$) change, or ceramide species or reactive oxygen species levels; (*d*) whether cytotoxicity was enhanced by L-*threo*-dihydrosphingosine (safingol); (*e*) whether physiological hypoxia increased acid ceramidase (AC) expression; and (*f*) the effect of the AC inhibitor *N*-oleoyl-ethanolamine (NOE) on cytotoxicity and ceramide species. Ceramide species were quantified by thin-layer chromatography and scintillography. Cytotoxicity was measured by a fluorescence-based assay using digital imaging microscopy (DIMSCAN). Gene expression profiling was performed by oligonucleotide array analysis. We observed, in 12 cell lines tested in normoxia (20% O_2), that the mean 4-HPR LC_{99} (the drug concentration lethal to 99% of cells) = 6.1 ± 5.4 μM (range, 1.7–21.8 μM); safingol (1–3 μM) synergistically increased 4-HPR cytotoxicity and reduced the mean 4-HPR LC_{99} to 3.2 ± 1.7 μM (range, 2.0–8.0 μM; combination index < 1). 4-HPR increased ceramide species in the three cell lines tested (up to 9-fold; $P < 0.05$). Hypoxia (2% O_2) reduced ceramide species increase, $\Delta\Psi_m$ loss, reactive oxygen species increase ($P < 0.05$), and 4-HPR cytotoxicity ($P = 0.05$; 4-HPR LC_{99}, 19.7 ± 23.9 μM; range, 2.3–91.4). However, hypoxia affected 4-HPR + safingol cytotoxicity to a lesser extent ($P = 0.04$; 4-HPR LC_{99}, 4.9 ± 2.3 μM; range, 2.0–8.2). Hypoxia increased AC RNA expression; the AC inhibitor NOE enhanced 4-HPR-induced ceramide species increase and cytotoxicity. The antioxidant *N*-acetyl-L-cysteine somewhat reduced 4-HPR cytotoxicity but did not affect ceramide species increase. We conclude the following: (*a*) 4-HPR was active against ESFT cell lines *in vitro* at concentrations achievable clinically, but activity was decreased in hypoxia; and (*b*) combining 4-HPR with ceramide modulators synergized 4-HPR cytotoxicity in normoxia and hypoxia.

INTRODUCTION

Ewing's sarcoma (ES) and peripheral primitive neuroectodermal tumors (PNETs) are small round blue cell tumors of childhood grouped together as the ES family of tumors (ESFT). They are linked by a common chromosomal translocation and similar profiles of proto-oncogene expression and may arise in bone or soft tissue (1, 2). ES and PNET are currently regarded as variants of the same neuroepithelial-derived tumor and show similar patterns of response to chemotherapeutic agents; hence, they are treated in a uniform manner. High-risk ESFT patients (metastatic disease, tumor volume > 200 ml, pelvic disease, age > 10 years) do poorly despite intensive chemotherapy and autologous bone marrow transplant, with long-term event-free survival of <40% (3).

Retinoids are natural or synthetic derivatives of vitamin A that have been shown to be important modulators of cellular growth and differentiation (4). Treating high-risk neuroblastoma patients with the differentiating retinoid 13-*cis*-retinoic acid in minimal residual disease (MRD) after myeloablative therapy supported by purged autologous bone marrow transplant significantly increased event-free survival (5). These results suggest that a similar MRD-targeted approach may benefit other pediatric solid tumors. The synthetic, p53-independent, cytotoxic retinoid *N*-(4-hydroxyphenyl) retinamide (4-HPR; fenretinide) has been shown to inhibit carcinogenesis in animal cancer models and is cytotoxic for a variety of different types of tumor cell lines *in vitro*, including neuroblastoma (4, 6). 4-HPR increased reactive oxygen species (ROS) in some tumor cell lines (6–9), and antioxidants inhibited 4-HPR-induced apoptosis in certain cell lines, implicating ROS as one mechanism of action of 4-HPR (7, 9). 4-HPR-induced cytotoxicity is receptor independent, and partially caspase independent (6, 10). Clinically, low-dose oral 4-HPR (1–3 μM serum levels) has been studied as a chemopreventive agent in breast, bladder, and oral cavity cancers, and it has shown minimal systemic toxicity (11). Pediatric Phase I trials of oral 4-HPR achieved 7–13 μM steady-state plasma levels with minimal hematological toxicity (12, 13), suggesting that 4-HPR, like 13-*cis*-retinoic acid, is potentially usable soon after myeloablative therapy.

Ceramides have been implicated in tumor cell death induced by 4-HPR (6, 14–16). Ceramides are a class of lipid second messengers involved in the regulation of diverse cellular responses, including cell death. Saturated sphinganine-backboned (or dihydroceramides) and desaturated sphingosine-backboned ceramides are generated sequentially by *de novo* synthesis. Ceramides can also derive from sphingomyelin breakdown via the activation of various sphingomyelinases by diverse stimuli, such as drugs, ionizing radiation, UV-C radiation, heat shock, oxidative stress, or the activation of cell surface receptors, such as tumor necrosis factor or CD95/Fas/APO-1 (16–18). However, it is not clear that all intracellular ceramide species pools are biologically equivalent. Ceramides have been reported to initiate apoptosis under hypoxic conditions in a p53-independent manner via caspase-3 activation and cause the activation of the pro-death c-Jun-NH_2-terminal kinase/stress-activated protein kinase cascade (19). Many ceramide species can be metabolized to less toxic forms by glucosylation and acylation via glucosylceramide synthase and 1-*O*-acylceramide synthase (20–22) or deacylated by ceramidases to sphingosine (23), which can be phosphorylated to spingosine-1-phosphate (16). Cyto-

Received 2/6/04; revised 5/5/04; accepted 5/20/04.

Grant support: Grants from the Children's Cancer Research Fund (S. Batra); Neil Bogart Memorial Laboratories of the T. J. Martell Foundation for Leukemia, Cancer, and AIDS Research (C. P. Reynolds and B. J. Maurer); the Wright Foundation (B. J. Maurer); The Chris Carrey Charitable Fund of the Stop Cancer Foundation (C. P. Reynolds and B. J. Maurer); the University of Southern California-Children's Hospital of Los Angeles Institute for Pediatric Clinical Research (C. P. Reynolds and B. J. Maurer); and National Cancer Institute Grant UO1CA88199 (T. J. Triche). Certain intellectual property rights pertaining to the contents of this report may be retained by the Children's Hospital of Los Angeles.

The costs of publication of this article were defrayed in part by the payment of page charges. This article must therefore be hereby marked *advertisement* in accordance with 18 U.S.C. Section 1734 solely to indicate this fact.

Note: S. Batra is currrently in the Division of Hematology-Oncology and Department of Pediatrics, Children's Memorial Hospital, Robert H. Lurie Cancer Center of Northwestern University, Northwestern University, Feinberg School of Medicine, Chicago, IL.

Requests for reprints: Barry J. Maurer, Division of Hematology-Oncology, MS #57, Children's Hospital Los Angeles, 4650 Sunset Boulevard, Los Angeles, CA 90027. Phone: (323) 669-5663; Fax: (323) 664-9455; E-mail: bmaurer@chla.usc.edu.

toxicity for a variety of solid tumor and leukemia cell lines (but not for nonmalignant cells) can be synergistically enhanced by combining 4-HPR with L-*threo*- dihydrosphingosine (safingol) or with inhibitors of glucosylceramide and/or 1-*O*-acylceramide synthase (14, 15).

We examined the cytotoxic properties of 4-HPR in human ESFT cell lines and determined the following: (*a*) whether 4-HPR increased ceramide species or ROS production or decreased mitochondrial membrane potential transition ($\Delta\Psi_m$); (*b*) the effects of physiological hypoxia (pO_2, approximately 15 mm Hg = 2% oxygen) and the antioxidant *N*-acetyl-L-cysteine (NAC) on 4-HPR-induced cytotoxicity, ceramides, ROS generation, and $\Delta\Psi_m$; (*c*) the role of *de novo* ceramide synthesis in 4-HPR-induced ceramide species generation; (*d*) whether putative modulators of ceramide species metabolism or signal transduction, such as safingol, synergized 4-HPR cytotoxicity; and (*e*) the transcriptional response of an ESFT cell line (SK-N-MC) to 4-HPR in both 20% oxygen (normoxia) and hypoxia, using expression profiling, to identify novel targets to further increase 4-HPR cytotoxicity in hypoxia.

MATERIALS AND METHODS

Cell Culture. The human PNET cell line SK-N-MC (24) was purchased from the American Type Culture Collection (Manassas, VA). The PNET cell line CHP-100 (25) was obtained from Dr. A. Evans, and ES cell lines TC-106, TC-71, TC-32, 5838, 9423, and A4573 were obtained from Dr. Timothy J. Triche (25, 26). These cell lines were maintained in RPMI 1640 supplemented with 10% heat-inactivated fetal bovine serum (complete medium) at 37°C in a humidified incubator containing 95% room air plus 5% CO_2 atmosphere. Cells were detached without trypsin from culture plates with modified Puck's Solution A plus EDTA (Puck's EDTA), which contains 140 mM NaCl, 5 mM KCl, 5.5 mM glucose, 4 mM $NaHCO_3$, 0.8 mM EDTA, 13 μM phenol red, and 9 mM HEPES buffer (pH 7.3). The human ESFT cell lines CHLA-9, CHLA-10, CHLA-32, and CHLA-258 were established in our laboratory (C. P. R.). The cell line CHLA-9 was established at diagnosis from a 14-year-old female with a thoracic PNET; CHLA-10 was established from the same patient after four cycles of induction chemotherapy with cisplatin, doxorubicin, cyclophosphamide, and etoposide. The CHLA-32 cell line was established at diagnosis from a 14-year-old male with a high-risk pelvic ES. The PNET cell line CHLA-258 was established from a distant relapse (solitary lung nodule) that occurred after induction and myeloablative chemotherapy (melphalan, carboplatin, and etoposide) in a 12-year-old female with paraspinal PNET. These cell lines were maintained in Iscove's Modified Dulbecco's Medium supplemented with 0.7 mM L-glutamine, insulin, and transferrin (5 μg/ml each), selenium (5 ng/ml), and 20% heat-inactivated fetal bovine serum (whole medium). Cell lines were studied during passages 5–20 and cultured at 37°C in a humidified incubator containing 95% room air plus 5% CO_2 atmosphere.

For cytotoxicity assays (described below) under 2% oxygen conditions, cells were seeded into 96-well plates and treated as described previously (6).

Drugs and Reagents. 4-HPR, safingol and melphalan were obtained from the National Cancer Institute (Bethesda, MD). Etoposide was obtained from Bristol-Myers Squibb Co. (Princeton, NJ). NAC, eosin Y, TLC-grade organic solvents, L-cycloserine, and fumonisin B_1 were purchased from Sigma Chemical Co. (St. Louis, MO). The pan-caspase enzyme inhibitor BOC-d-fmk was from Enzyme Systems Products (Livermore, CA). Ecolume scintillation mixture was from ICN Biomedicals (Costa Mesa, CA). [9,10-^{3}H(*N*)]Palmitic acid (50 Ci/mmol) was from Dupont NEN Research Products (Boston, MA). Iscove's Modified Dulbecco's Medium was from BioWhittaker (Walkersville, MD). RPMI 1640, fetal bovine serum, and L-glutamine were from Gemini BioProducts (Calabasas, CA). ITS Premix culture supplement (insulin, transferrin, and selenious acid) was from Collaborative Biomedical Products (Bedford, MA). Fluorescein diacetate was from the Eastman Kodak Company (Rochester, NY). 5-(and -6)-carboxy-2′,7′-dichlorofluorescein diacetate (carboxy-DCFDA) and the fluorescent probe JC-1 were from Molecular Probes (Eugene, OR). Stock solutions of fluorescein diacetate (1 mg/ml), carboxy-DCFDA (10 mM), and JC-1 (2 mg/ml) were dissolved in DMSO and stored at −20°C (fluorescein diacetate and JC-1) or in liquid nitrogen vapor (carboxy-DCFDA).

Cytotoxicity Assay. Cytotoxicity of drugs was determined using the fluorescence-based DIMSCAN assay (14, 15, 27–29),[6] which uses digital imaging microscopy to quantify viable cells that selectively accumulate fluorescein diacetate. DIMSCAN is capable of measuring cytotoxicity over a 4–5-log dynamic range. Briefly, cells were seeded into 96-well plates at 2,500–10,000 cells/well (lower cell numbers were used for more rapidly proliferating cell lines) in 150 μl of complete medium per well. Cells were allowed to attach overnight before the addition of 4-HPR (0, 2, 4, 8, and 12 μM final drug concentrations) and/or safingol (4-HPR:safingol molar ratio, 4:1) and/or NAC and/or BOC-d-fmk and/or *N*-oleoyl-ethanolamine (NOE) in 50-μl volumes of whole medium to various final drug concentrations, in replicates of 12 wells per concentration. Plates were assayed at 4 days (or at 7 days for CHLA-258 and CHLA-32) after initiation of drug exposure to allow for maximum cell death and outgrowth of surviving cells. The pan-caspase inhibitor BOC-d-fmk was used to block the apoptotic component of cell death in SK-N-MC cells. Cells were preincubated for 8 h with 40 μM BOC-d-fmk (6) before and daily after the addition of 4-HPR (2–8 μM) or 4-HPR + safingol (4:1 molar ratio) and assayed by DIMSCAN at +96 h to assess the effect of caspase inhibition on viability. Results were analyzed and expressed as the fraction of treated cells surviving compared with controls using Excel software (Microsoft, Seattle, WA) and graphed using SigmaPlot 6.0 (Jandell Scientific, San Rafael, CA). Limits of detection were determined by the estimated number of cells present in control wells at the time that they were treated with drug, generally targeted at 10^4 cells, giving a detection limit for cytotoxicity of $\sim 10^{-4}$. The stability of 4-HPR, safingol, L-cycloserine, fumonisin B_1, NAC, BOC-d-fmk, or NOE for 4–7 days in the DIMSCAN cytotoxicity assay system is not known. Control cells were treated with vehicle solvents of 0.1% ethanol (4-HPR) and/or 0.2% DMSO (BOC-d-fmk).

Lipid Analysis. Methods were modified from Lavie *et al.* (30), as described previously (14, 15). Briefly, cells were seeded into 6-well plates (5×10^5 cells/well in 2 ml of whole medium) and allowed to recover overnight. All drug-treated or control samples were done in triplicate. At zero time, [^{3}H]palmitic acid (1 μCi/ml medium) and drug(s) or ethanol (control) were added. Lipids were extracted from cells (drug-treated and control cells) at +6 h and +24 h, stored at −20°C, and analyzed by TLC. Changes in ceramide species level are expressed as the mean fold-increase in drug-treated samples as compared with matched controls. The sphinganine *N*-acyltransferase (dihydroceramide synthase) inhibitor fumonisin B_1 (31) was added 16 h before the addition of other drugs to a final concentration of 90 μM. The serine palmitoyltransferase inhibitor L-cycloserine (31) was added 3 h before the addition of other drugs to a final concentration of 1 mM. NAC was added to a concentration of 1 mM 3 h before the addition of 4-HPR. Drugs did not affect [^{3}H]palmitic acid uptake. The TLC system used did not resolve saturated *N*-acylsphinganines (dihydroceramides) and unsaturated *N*-acylsphingosines (ceramides). After common usage, *N*-acylsphinganines and *N*-acylsphingosines will both be termed "ceramide species" in this article.

Measuring Apoptosis. To quantify the apoptotic cells with sub-G_1-G_0 DNA content, 2×10^6 SK-N-MC cells were cultured in 25-cm^2 flasks with or without 4-HPR (8 μM), safingol (2 μM), or 4-HPR (8 μM) + safingol (2 μM) for 6 and 24 h in both normoxia (20% O_2) and hypoxia (2% O_2). Cells were harvested, washed in PBS, centrifuged, and resuspended in 1 ml of 0.1% sodium citrate containing 0.05 mg/ml propidium iodide for 10 min on ice, and then RNase (50 μg) was added for 30 min at room temperature in the dark. DNA content was measured on a Coulter Epics flow cytometer using a 488 nm argon laser and a 610 ± 10 nm band pass filter (32). Experiments were done in triplicate.

ROS. SK-N-MC cells (2×10^6 cells in 5 ml of complete medium per 25-cm^2 flask) were incubated for 6 h with or without 4-HPR (10 μM) in 20% O_2 or 2% O_2. Medium was discarded and replaced with carboxy-DCFDA (50 μM) for 20 min at 37°C. Cells were harvested, transferred to foil-wrapped tubes, and analyzed immediately by flow cytometry using a 525 ± 10 nm band pass filter. As a positive control, cells were loaded with carboxy-DCFDA for 20 min as described above, the medium was discarded, and hydrogen peroxide (100 μM in medium without fetal bovine serum) was added for 15 min before harvesting for flow cytometry (6). Experiments were done in triplicate.

[6] www.DIMSCAN.com.

Mitochondrial Membrane Potential Transition. The $\Delta\Psi_m$ was measured in 1×10^6 SK-N-MC cells cultured in 6-well plates at 6 and 24 h after incubation with 4-HPR (10 μM) in 20% O_2 and 2% O_2 using JC-1 (10 μg/ml for 10 min at 37°C) probe by flow cytometry (33). JC-1 is a cationic dye that accumulates in the mitochondria, depending on mitochondrial membrane potential. This accumulation is indicated by a fluorescence emission shift from green (525 ± 10 nm) to red (601 ± 10 nm).

Western Blot Analysis. Cells (2×10^6) cultured in 25-cm^2 flasks were lysed in radioimmunoprecipitation assay buffer (34), and 40 [for p53, MDM2, caspase 3, bcl-2, bax, and poly(ADP-ribose) polymerase (PARP) protein assays] or 60 μg (for p21 protein assay) of total protein were loaded for each lane. Proteins were fractionated on 12–14% Tris-glycine pre-cast gels (Novex, San Diego, CA), transferred to nitrocellulose membrane (Protan, Keene, NH), and hybridized with primary antibodies followed by horseradish peroxidase-conjugated secondary antibodies. The p53 mouse monoclonal antibody (DO-1), p21 rabbit polyclonal antibody (C-19), MDM2 mouse monoclonal antibody (SMP14), bax rabbit polyclonal antibody (P-19), bcl-2 mouse monoclonal antibody (SC-509), caspase-3 rabbit polyclonal antibody (H-277), PARP rabbit polyclonal antibody (H-250), actin goat polyclonal antibody (C-11), and horseradish peroxidase-conjugated secondary antimouse, antigoat, and antirabbit antibodies were purchased from Santa Cruz Biotechnology, Inc. (Santa Cruz, CA). Proteins were visualized using ECL Western blotting reagent (Amersham Pharmacia Biotech, Piscataway, NJ). As a control, the induction of p53, p21, and MDM2 proteins (the latter two as indicators of p53 function) was analyzed 16 h after the addition of melphalan (6 μg/ml). A cell line was defined to have p53 function if there was a >1.2-fold induction of p21 and MDM2 protein (34). Caspase 3, bcl-2, and bax protein levels and PARP protein cleavage were analyzed at 8–24 h after addition of 4-HPR (10 μM), with or without safingol (2.5 μM), in SK-N-MC cells. Bands were quantified using densitometry on the Eagle Eye II still video system using Eagle Sight software version 3.22 (Stratagene, Cedar Creek, TX) and normalized to actin (loading control).

Northern Blot Analysis. RNA was extracted using the TRIZOL reagent (Life Technologies, Inc., San Diego, CA) and purified using Qiagen RNAeasy kit (Qiagen, Valencia, CA). For reverse transcription-PCR, 1 μg of total RNA/sample was reverse-transcribed to cDNA, using the Superscript reverse transcription-PCR kit (PE Applied Biosystems, Foster City, CA). The human acid ceramidase (AC) cDNA fragment was amplified by PCR (an initial 95°C for 5 min, then 94°C for 1 min, 51°C for 1 min and 72°C for 1 min, 40 cycles), using the following primer pairs: F554, 5′-TGATACCTGGGTCATAACTGAGC-3′; and R1079, 5′-ATTCTCTTGGCTGGTGCGG -3′. Ten μg of total RNA were fractionated on a 1% formaldehyde gel, transferred onto a nylon membrane (Hybond N; Amersham Pharmacia Biotech), and probed with ^{32}P-labeled human AC and β-actin cDNA fragments using previously described methods (35). RNA bands were quantified using densitometry.

Oligonucleotide Array Analysis. Total RNA was extracted from 2×10^6 SK-N-MC cells after 24 h of 4-HPR (10 μM) treatment in 20% O_2 and 2% O_2. cDNA and cRNA synthesis and hybridization to HG U95A oligonucleotide arrays (Affymetrix) and analysis of the data were performed according to previously published methods (36).

Dye Exclusion Cell Viability Assay. The trypan blue exclusion was performed on 8×10^4 cells seeded in triplicate in 24-well plates at different time points with 4-HPR (10 μM) and/or cycloserine (1 mM) and/or fumonisin B (90 μM). The cells were suspended in a 0.4% trypan blue solution and counted with a hemocytometer.

Statistical Analysis. Cytotoxicity, ROS, apoptosis, and lipid data are presented as means ± 95% confidence interval. The 95% confidence interval was calculated as $1.96\sigma/\sqrt{n}$, where σ = SD of ungrouped data, and n = number of trials. The statistical significance (of differences in means) was evaluated by the unpaired, two-sided Student's t test using Microsoft Excel 97 software (Redmond, WA). Drug-induced cytotoxic synergy was analyzed by the combination index (CI) method of Chou (37, 38) and expressed as the CI at the LC_{99} (the drug concentration lethal to 99% of cells). Synergism is defined as a greater than additive effect, and antagonism is defined as a less than additive effect. By this method, CI = 1 indicates an additive effect, CI < 1 indicates synergy, and CI > 1 indicates antagonism. Using CalcuSyn software, synergy is further refined as synergism (CI = 0.3–0.7), strong synergism (CI = 0.1–0.3), and very strong synergism (CI < 0.1; Ref. 37).

RESULTS

4-HPR Cytotoxicity. 4-HPR was cytotoxic for ESFT cell lines but was antagonized by hypoxia in ESFT cell lines. The mean 4-HPR LC_{99} for 12 ESFT cell lines under normoxic (20% O_2) conditions was 6.1 ± 5.4 μM (range, 1.7–21.8 μM). However, hypoxic conditions (2% O_2) diminished the sensitivity of ESFT cell lines to 4-HPR, increasing the mean LC_{99} to 19.7 ± 23.9 μM (range, 2.3–91.4 μM; $P = 0.03$; Table 1). The mean log cell kill of 4-HPR (8 μM) in normoxia was 2.4 ± 1.1 but decreased to 1.5 ± 0.9 under hypoxic conditions ($P = 0.005$; Table 1). Representative drug cytotoxicity dose-response curves are shown in Fig. 1*A*. 4-HPR (10 μM) in 20% O_2 increased the apoptotic population (sub-G_0-G_1 DNA content in SK-N-MC cells) to 68.8 ± 3.4% at +24 h, compared with 10.2 ± 3.1% in controls ($P < 0.001$), whereas the apoptotic fraction of 4-HPR-treated cells was reduced to 33.4 ± 3.9% in hypoxic conditions ($P < 0.001$). Representative flow cytometry histograms are presented in Fig. 1*B*.

Western Blot Analysis of p53, p21, and MDM2 Expression. To determine the relationship of 4-HPR cytotoxicity to p53 function in ESFT, the basal and induced protein levels of p53, p21, and MDM2 (the latter two as indices of p53 function) at +16 h after addition of melphalan (6 μg/ml; Ref. 34) were analyzed by immunoblotting (data not shown). We determined that p21 and MDM2 expression was inducible (≥1.2-fold) in seven cell lines (CHLA-9, TC-106, 5838, 9423, CHLA-32, A4573, and CHP-100). A failure to induce p21, and MDM2 (≤1.2-fold) was observed in five cell lines (CHLA-10, CHLA-258, TC-32, TC-71, and SK-N-MC; Table 1).

Effect of Safingol on 4-HPR Cytotoxicity in ESFT Cell Lines. We determined the cytotoxicity of combining 4-HPR with safingol at a 4:1 molar ratio (4-HPR:safingol) in ESFT cell lines. In normoxia, safingol clearly synergized 4-HPR cytotoxicity in 10 of 12 cell lines over at least part of the dose range (Fig. 2; Table 2), whereas results trended toward additivity in two cell lines (TC-71 and 5838). In hypoxia, safingol clearly synergized 4-HPR cytotoxicity in 8 of 12 cell lines over at least part of the dose range (Fig. 2; Table 2), whereas results trended toward additivity in four cell lines (CHLA-9, TC-106, TC-71, and 5838). The combination of 4-HPR + safingol achieved multilog cell killing in ESFT cell lines (Fig. 2), even in multidrug-resistant, p53 nonfunctional cell lines established at relapse after intensive multiagent chemotherapy, such as CHLA-10 and CHLA-258 (39). The mean log cell kill caused by 4-HPR (8 μM) + safingol

Table 1 *4-HPR[a] LC_{99} and log cell kill at (8 μM) 4-HPR in ESFT cell lines in normoxia and hypoxia*

Cells were exposed to 4-HPR, and cytotoxicity was assayed by DIMSCAN assay at +4 days (or +7 days for CHLA-258 and CHLA-32). LC_{99} is defined as the concentration of drug needed to kill 99% of cells. Normoxia = 20% oxygen; hypoxia = 2% oxygen, ~15–20 mm pO_2. Measurement of p53 function was by increase of p21 and MDM2 protein after 16 h of treatment with melphalan (6 μg/ml; Ref.. 34), indicated as follows: +, functional p53; and −, nonfunctional p53 .

		20% O_2		2% O_2	
Cell line	p53 function	LC_{99} (μM)	Log cell kill	LC_{99} (μM)	Log cell kill
TC-71	−	1.7	4.0	2.3	3.0
TC-106	+	3.4	2.4	4.6	2.6
5838	+	2.4	4.0	9.8	2.0
9423	+	7.3	1.4	19.9	1.0
CHLA-32	+	5.6	1.9	14.8	1.5
A4573	+	3.0	2.9	11.7	2.0
CHP-100	+	5.2	3.2	6.9	2.2
SK-N-MC	−	4.4	2.8	31.5	0.8
CHLA-9	+	4.0	2.3	15.5	2.0
CHLA-10	−	10.2	1.7	20.7	1.5
CHLA-258	−	21.8	0.3	91.4	0.0
TC-32	−	4.0	2.1	8.0	0.3
Mean ± SD		6.1 ± 5.4	2.4 ± 1.1	19.7 ± 23.9	1.5 ± 0.9
Range		1.7–21.8	0.3–4.0	2.3–91.4	0.0–3.0

[a] 4-HPR, *N*-(4-hydroxyphenyl) retinamide; ESFT, Ewing's family of tumors.

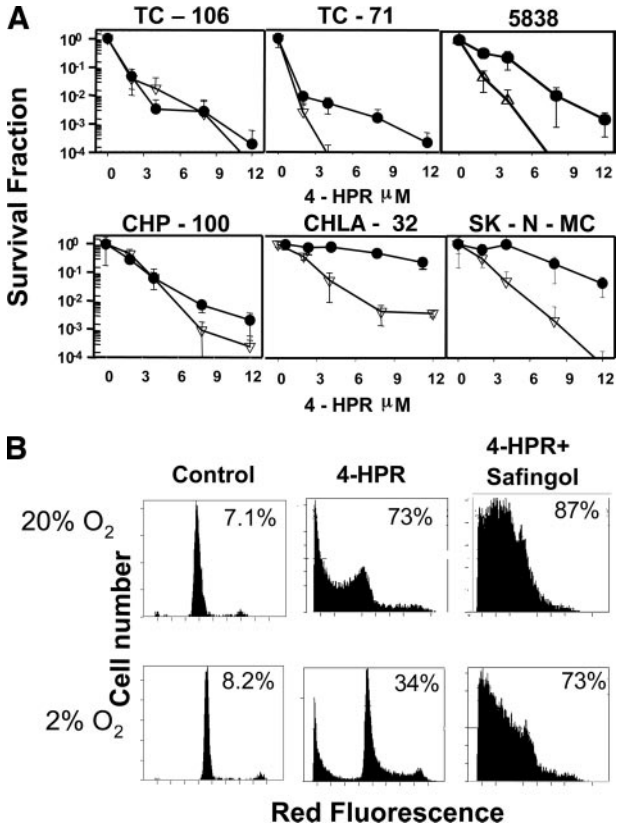

Fig. 1. *N*-(4-Hydroxyphenyl) retinamide (4-HPR) cytotoxicity was antagonized by hypoxia in Ewing's sarcoma family of tumors cell lines. *A*, dose-response of Ewing's sarcoma family of tumors cell lines to 4-HPR in normoxia (20% O_2; ▽) and hypoxia (2% O_2; ●). Cell lines were exposed to 4-HPR (0–12 μM), and cytotoxicity was assayed with a fluorescence-based assay using digital imaging microscopy (DIMSCAN) at +96 h (at +7 days for CHLA-32). *Bars* indicate 95% confidence intervals. *B*, effect of hypoxia on apoptosis induced by 4-HPR and 4-HPR + safingol. SK-N-MC cells were treated with 4-HPR (10 μM) or 4-HPR (10 μM) + safingol (2 μM) for 24 h and harvested, and apoptosis was detected by propidium iodide staining of DNA. The fluorescence intensity of 15,000 cells was analyzed using a flow cytometer. 4-HPR-induced apoptosis was decreased in hypoxia compared with that observed in 20% O_2 ($P < 0.001$). Apoptosis induced by 4-HPR + safingol was greater than that induced by 4-HPR-alone in both 20% and 2% O_2 ($P < 0.002$; *right panels*). Representative results from a single experiment ($n = 3$) are shown. The percentage of cells with a sub-G_1-G_0 (apoptotic) DNA content are shown. Data ± 95% confidence intervals and significance levels were calculated from triplicate samples.

(2 μM) in 20% O_2 was 3.6 ± 0.7, which modestly decreased ($P = 0.01$) to 3.0 ± 0.8 logs under hypoxic conditions (Table 2). Thus, 4-HPR + safingol retained multilog cytotoxicity ($P < 0.001$) even in 2% oxygen. Additionally, as shown in Fig. 1*B*, *middle* and *right panels*, at +24 h, the combination of 4-HPR + safingol caused more apoptosis in SK-N-MC cells than 4-HPR alone in both 20% O_2 (82.4 ± 5.6% *versus* 68.8 ± 5.6%; $P = 0.001$) and hypoxia (71.5 ± 2.9% *versus* 33.4 ± 3.9%; $P < 0.001$).

Hypoxia Decreased 4-HPR-Associated *de Novo* Ceramide Species and ROS Generation. To determine whether 4-HPR increased the level of ceramide species in ESFT cell lines, lipid extracts were prepared from 5838 (ES) and SK-N-MC (PNET) cells treated with increasing doses of 4-HPR (5, 10, and 15 μM) in both 20% O_2 and hypoxic conditions, and the sum of [^{3}H]palmitic acid-labeled saturated and desaturated ceramide species was quantified. In 5838 cells, 4-HPR increased ceramide species up to 5-fold at +6 h in a dose-dependent manner in 20% O_2 (Fig. 3*A*) and up to 9.4 ± 0.5-fold with 4-HPR (15 μM; $P < 0.01$) at +24 h. However, in 2% O_2, ceramide species in 4-HPR-treated 5838 cells at +6 h increased only 2-fold (Fig. 3*A*; $P < 0.03$). 4-HPR (15 μM) also induced a 3.0 ± 0.5-fold increase of glucosylceramide at +6 h in the 5838 cell line in 20% O_2 but only induced a 1.6 ± 0.1-fold increase in 2% O_2 ($P = 0.03$ compared with normoxia; data not shown). A similar pattern was observed in SK-N-MC cells (Fig. 3*B*), with the increase of 4-HPR-induced ceramide species at +24 h reduced in hypoxic conditions compared with 20% O_2 ($P < 0.02$). 4-HPR treatment induced an increase in ceramide species at +24 h in two of three additional cell lines [CHP-100, TC-106, and CHLA-258, 2.6 ± 0.6-fold ($P = 0.05$), 4.1 ± 1.5-fold ($P = 0.07$), and 0.8 ± 0.4-fold ($P = 0.8$) increases, respectively, compared with controls; data not shown). Overall, 4-HPR cytotoxicity was associated with an increase in ceramide species at +24 h in five of six cell lines analyzed (SK-N-MC, 5838, TC-71, CHP-100, TC-106, and CHLA-258).

4-HPR Increased Ceramide Species by *de Novo* Synthesis. To determine the origin of the ceramide species increased by 4-HPR, the effects of two inhibitors of *de novo* ceramide synthesis were assayed. L-Cycloserine is an inhibitor of serine palmitoyltransferase, the initial and rate-limiting step of *de novo* ceramide synthesis, whereas fumonisin B_1 is an inhibitor of (dihydro)ceramide synthase (31). In the SK-N-MC, 5838 (Fig. 3), and TC-71 cell lines (data not shown), 4-HPR treatment increased ($P < 0.01$) ceramide species at +6 and +24 h, whereas both inhibitors reduced or prevented 4-HPR-induced ceramide species increase at +6 and +24 h ($P < 0.01$; Fig. 3, *C–F*). Cell viability by trypan blue exclusion of SK-N-MC cells after exposure to 4-HPR (10 μM), with and without inhibitors, was also determined. Compared with controls (percentage of dead cells, 10.2 ± 3.0 at +6 h and 11.9 ± 8.1 at +24 h), 4-HPR treatment was significantly cytotoxic to SK-N-MC cells (percentage of dead cells, 47.8 ± 13.8 at +6 h, and 71.4 ± 3.0 at +24 h; $P < 0.001$). Cycloserine (1 mM) alone was cytotoxic to SK-N-MC cells compared with controls [percentage of dead cells, 9.9 ± 5.0 at +6 h ($P > 0.05$) and 21.8 ± 5.1 at +24 h ($P = 0.04$)] and also increased 4-HPR cytotoxicity (percentage of dead cells, 51.0 ± 1.9 at +6 h and 83.4 ± 4.5 at +24 h; $P < 0.001$). Single-agent fumonisin B (90 μM) was cytotoxic to SK-N-MC cells compared with controls (% dead cells = 11.4 ± 3.7, $P > 0.05$, and 29.1 ± 4.1, $P = 0.03$), and also increased 4-HPR cytotoxicity (percentage of dead cells, 40.4 ± 9.8 and 83.8 ± 4.8 at +6 and +24 h, respectively; $P < 0.001$). Because cycloserine and fumonisin B_1 were both cytotoxic to these cell lines as single agents, the effect of these ceramide synthesis inhibitors on that portion of 4-HPR cytotoxicity attributable to *de novo* ceramide synthesis could not be determined; however, these results indicate that the 4-HPR-mediated ceramide species increase was primarily from *de novo* synthesis. The possibility that a portion of the increase in ceramide species observed was due to either decreased metabolism of ceramides into sphingosine or reduced conversion of ceramides into sphingomyelin or other products was not excluded.

4-HPR-Induced Mitochondrial Membrane Potential Depolarization, bax Increase, and ROS Levels Were Decreased in Hypoxia. We also determined the mitochondrial membrane potential ($\Delta\Psi_m$) by JC-1 staining and flow cytometry in SK-N-MC cells treated with 4-HPR (10 μM) at +6 and +24 h in 20% and 2% O_2 (Fig. 4*A*, representative data from individual experiments are shown). In normoxia, 4-HPR significantly decreased $\Delta\Psi_m$ at +6 h (ratio of red to green fluorescence = 0.9 ± 0.1 compared with 3.3 ± 0.3 in controls; $P = 0.01$; Fig. 4*A*, *ii*) and at +24 h (ratio of red to green fluorescence = 0.03 ± 0.01 compared with 2.7 ± 0.2 in controls; $P = 0.002$; Fig. 4*A*, *v*). However, hypoxia blunted the 4-HPR-induced loss of $\Delta\Psi_m$ at both +6 h (ratio of red to green fluorescence = 2.1 ± 0.3; $P = 0.02$; Fig. 4*A*, *iii*) and +24 h (ratio of red to green fluorescence = 0.2 ± 0.05; $P = 0.03$; Fig. 4*A*, *vi*), compared with normoxia.

4-HPR is known to generate ROS in certain tumor cell types (6–9). We analyzed the effects of hypoxia and the thiol antioxidant NAC on 4-HPR-induced ROS levels and the effects of NAC on 4-HPR-

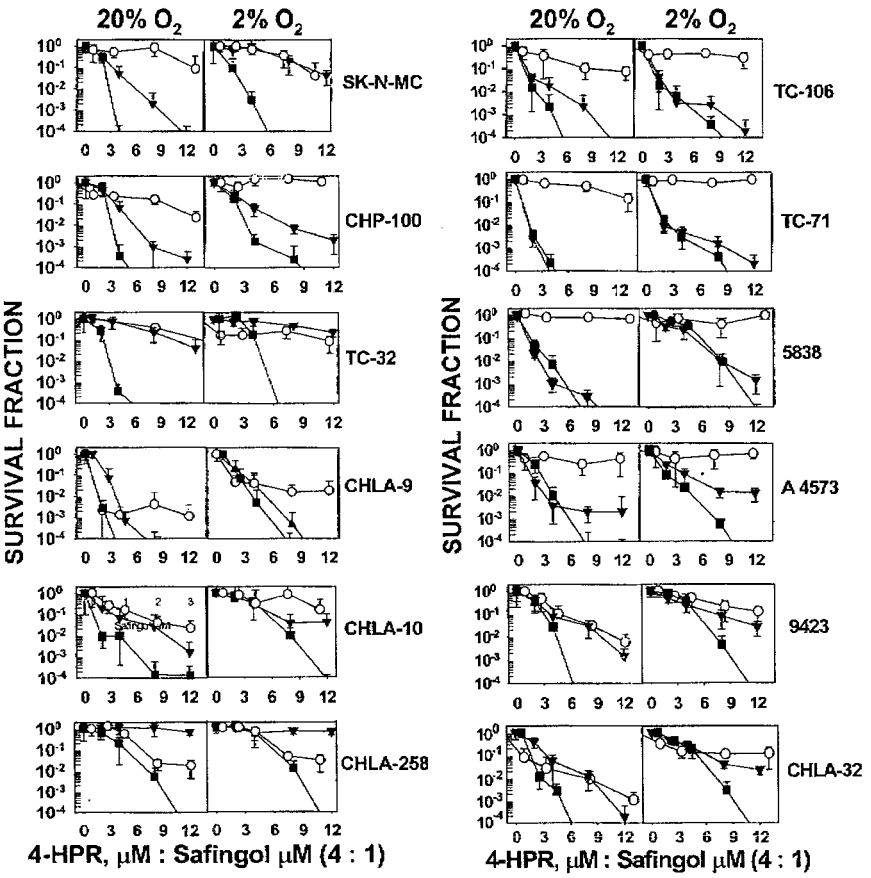

Fig. 2. Cytotoxicity of *N*-(4-hydroxyphenyl) retinamide (4-HPR), safingol, and 4-HPR + safingol in Ewing's sarcoma family of tumors cell lines in normoxia and hypoxia. Dose-responses of 12 Ewing's sarcoma family of tumors cell lines assayed in normoxia (20% O_2) and hypoxia (2% O_2) to 4-HPR (▼), safingol (○), or 4-HPR + safingol (4:1 molar ratio; ■) were assessed using the DIMSCAN assay. Cytotoxicity was assayed at +96 h (at +7 days for CHLA-258 and CHLA-32). Representative data from single experiments are shown. The combination of 4-HPR + safingol induced multilog cell killing in all cell lines under both normoxic and hypoxic conditions. Individual LC_{99} values and combination index values as a measure of synergy are tabulated in Tables 1 and 2.

mediated ceramide species generation and cytotoxicity (Fig. 4*B*). 4-HPR caused an increase in ROS (flow cytometry mean fluorescence in arbitrary units) compared with controls (383.6 ± 3.8 *versus* 294 ± 21; $P = 0.03$) in SK-N-MC cells at +6 h (Fig. 4*B*, *ii*). However, both NAC (327.5 ± 8.5; $P = 0.01$; Fig. 4*B*, *iii*) and hypoxia (368 ± 5; $P = 0.04$; Fig. 4*B*, *iv*) blunted the ROS increase compared with normoxic conditions. Interestingly, 4-HPR-induced ceramide species were not decreased ($P = 0.2$) in the presence of NAC (Fig. 4*C*), suggesting that ceramide species increase was independent of ROS increase. Additionally, cycloserine (1 mM) did not prevent 4-HPR-generated ROS (data not shown) at +6 h but did prevent an increase of ceramide species (Fig. 3, *D* and *F*). Together, these data suggest that increases of ROS and ceramide species are independent effects in EFST cell lines. The cytotoxicity of 4-HPR was decreased somewhat by NAC (molar ratio of 4-HPR to NAC, 1:40) at 4-HPR concentrations of ≥10 μM ($P = 0.01$), but multilog cytotoxicity was retained in the presence of NAC (Fig. 4*D*), suggesting that ROS was not responsible for the majority of the 4-HPR cytotoxicity observed.

There are conflicting reports of the caspase dependence of 4-HPR cytotoxicity (6, 40). We determined whether 4-HPR and 4-HPR + safingol cytotoxicity was caspase dependent in SK-N-MC cells. In SK-N-MC cells, daily addition of the pan-caspase inhibitor BOC-d-fmk to 4-HPR-treated cells only minimally decreased the cytotoxicity of 4-HPR (survival fraction increased from ~1% to ~15%) and 4-HPR + safingol (survival fraction increased from <0.1% to ~1%; Fig. 5*A*). These data suggest that the mode of cell death induced by 4-HPR and 4-HPR + safingol is mainly caspase independent in SK-N-MC cells.

We also determined the effect of hypoxia on 4-HPR-induced protein levels of activated caspase-3, bax, bcl-2, and PARP protein cleavage (10, 40, 41). SK-N-MC cells exposed to 4-HPR at +24 h evidenced caspase-3 activation (data not shown), an increase of bax protein (Fig. 5*B*, 6-fold increase in normoxia, normalized to actin, *middle panel*), and cleavage of PARP protein (Fig. 5*B*, *bottom panel*). Under hypoxic conditions, bax protein level only increased 3-fold (Fig. 5*B*, *middle panel*, *Lane 4*). Bcl-2 protein level was not changed by treatment in normoxia or hypoxia (Fig. 5*B*, *top panel*). 4-HPR (10 μM) + safingol (2.5 μM) also increased bax protein, PARP cleavage (Fig. 5*B*), and caspase-3 activation (data not shown) at +24 h. Increase of bax protein (2.5-fold and 5.9-fold) in normoxia (*N*) was

Table 2 *Cytotoxicity of 4-HPR[a] + safingol for ESFT cell lines in normoxia and hypoxia*

Cytotoxicity of 4-HPR (8 μM) + safingol (2 μM) (4:1 molar ratio) for ESFT cell lines measured in normoxia (20% O_2) and hypoxia (2% O_2) by DIMSCAN assay at +4 days (or +7 days for CHLA-258 and CHLA-32). Synergy was assessed by CI analysis calculated at LC_{99} values. CI = 0.1–0.3 (strong synergism); CI = 0.3–0.7 (synergism); CI = 0.7–0.9 (slight synergism); CI = 0.9–1.1 (additive); CI > 1.1 (antagonism).

	20% O_2		2% O_2	
Cell line	Log cell kill (H+S)	CI	Log cell kill (H+S)	CI
TC-71	4.0	0.8	3.2	0.7
TC-106	4.0	0.2	3.5	0.6
5838	3.6	0.8	2.0	0.7
9423	4.0	0.7	2.5	0.8
CHLA -32	4.0	0.4	2.5	0.6
A4573	3.5	0.5	4.0	0.5
CHP-100	4.0	0.5	3.7	0.4
SK-N-MC	4.0	0.4	4.0	0.3
CHLA-9	4.0	1.0	2.5	0.7
CHLA-10	4.0	0.3	4.0	0.2
CHLA-258	2.4	0.4	2.0	0.9
TC-32	2.1	0.1	1.8	<0.1
Mean ± SD	3.6 ± 0.7	0.5	3.0 ± 0.8	0.5

[a] 4-HPR, *N*-(4-hydroxyphenyl) retinamide; ESFT, Ewing's family of tumors; CI, combination index; H+S, 4-HPR + safingol.

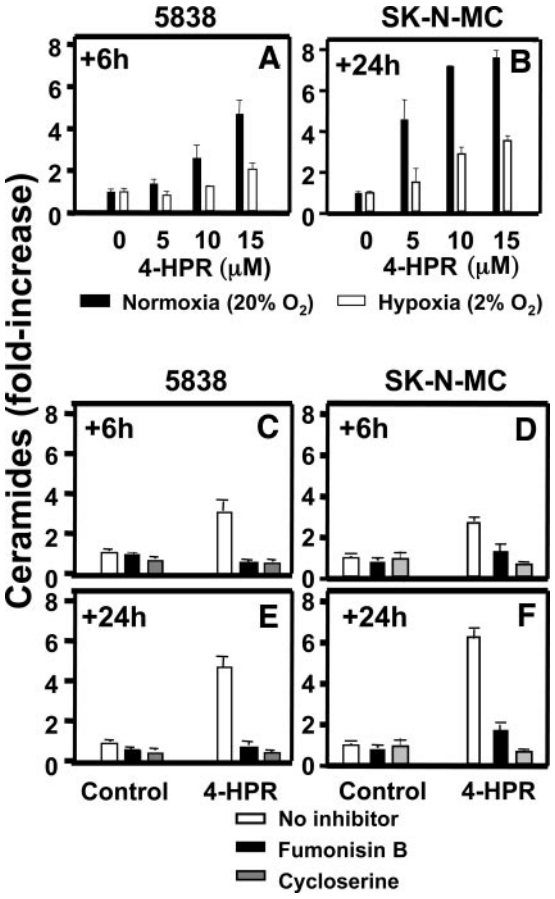

Fig. 3. Effect of hypoxia and inhibitors of *de novo* ceramide synthesis on *N*-(4-hydroxyphenyl) retinamide (4-HPR)-induced ceramide species increase in Ewing's sarcoma family of tumors cell lines. Cells were exposed to drug and [^{3}H]palmitic acid, and lipids were assayed. Results are expressed as the fold increase in ^{3}H-labeled ceramide species over controls. *A*, increase of ceramide species in 20% O_2 (■) of 5838 cells exposed to 4-HPR (5, 10, and 15 μM) for 6 h. Labeled ceramide species increased 1.4 ± 0.2-fold ($P = 0.1$), 2.6 ± 0.6-fold ($P = 0.05$), and 4.7 ± 0.7-fold ($P = 0.008$), respectively, over control levels. Compared with 20% O_2, 4-HPR-induced ceramide species increased less in 2% O_2 (□) [0.9 ± 0.1-fold ($P = 0.02$), 1.2 ± 0.0-fold ($P = 0.03$), and 2.0 ± 0.3-fold ($P = 0.01$), respectively]. *B*, increase of ceramide species in 20% O_2 (■) of SK-N-MC cells exposed to 4-HPR (5, 10, and 15 μM) for 24 h. Labeled ceramide species increased 4.5 ± 0.9-fold ($P = 0.006$), 7.2 ± 0.1-fold ($P = 0.005$), and 7.6 ± 0.3-fold ($P = 0.004$), respectively. Compared with 20% O_2, 4-HPR-induced ceramide species increased less in 2% O_2 (□) [1.5 ± 0.7-fold ($P = 0.003$), 2.9 ± 0.3-fold ($P = 0.01$), and 3.5 ± 0.2-fold ($P < 0.001$), respectively]. *C*–*F*, increase of labeled ceramide species at +6 h and +24 h in 5838 (*C* and *E*) and SK-N-MC (*D* and *F*) cells exposed to 4-HPR (10 μM) ± L-cycloserine (1 mM) or fumonisin B_1 (90 μM) in 20% O_2. *White bars* are ethanol-treated controls or 4-HPR alone. *Black bars* represent ethanol + L-cycloserine (controls) or 4-HPR + L-cycloserine. *Gray bars* represent ethanol + fumonisin B_1 (controls) or 4-HPR + fumonisin B_1. L-Cycloserine is an inhibitor of serine palmitoyltransferase, the rate-limiting enzyme of *de novo* ceramide synthesis. Fumonisin B is an inhibitor of (dihydro)ceramide synthase. Both L-cycloserine and fumonisin B_1 substantially prevented increase of labeled ceramide species by 4-HPR ($P < 0.01$) in both cell lines at +6 h and +24 h, indicating that 4-HPR increased ceramide species by *de novo* synthesis (note that ceramide species includes dihydroceramides; see "Materials and Methods").

reduced in hypoxia (*H*; 1.9-fold and 2.9-fold) at +8 and +24 h, respectively (+8 h data not shown).

Transcriptional Response to Hypoxia. Having observed that hypoxia decreased 4-HPR cytotoxicity in SK-N-MC cells, we sought a mechanism that may be associated with hypoxia-induced decrease of 4-HPR cytotoxicity in this cell line. Using oligonucleotide microarrays (Affymetrix), the gene expression profiles of SK-N-MC cells at +24 h in both normoxia and hypoxia, with and without 4-HPR treatment, were determined. Of the 12,600 genes examined, ~400 genes were either induced or down-regulated >2-fold compared with controls (data not shown). Among these, RNA expression of the AC gene was increased 2.1-fold in cells treated for 24 h with 4-HPR in hypoxia, as compared with normoxia. Northern blot analysis (Fig. 6*B*) validated this finding.

Effect of NOE on 4-HPR Cytotoxicity and Ceramide Species in SK-N-MC Cells. Having determined that hypoxia induced an increase in AC RNA levels, which potentially explained the decreased levels of 4-HPR-induced ceramide species and cytotoxicity observed, we determined the effect on cytotoxicity of combining 4-HPR with the AC inhibitor NOE (42, 43) at a 1:3 molar ratio (4-HPR:NOE) in SK-N-MC cells. Addition of NOE significantly synergized 4-HPR cytotoxicity in SK-N-MC cells and achieved multilog cell killing in both 2% O_2 (CI < 0.1) and 20% O_2 (CI = 0.1) at +96 h (Fig. 6*C*). To determine whether NOE enhanced the 4-HPR-induced increase of

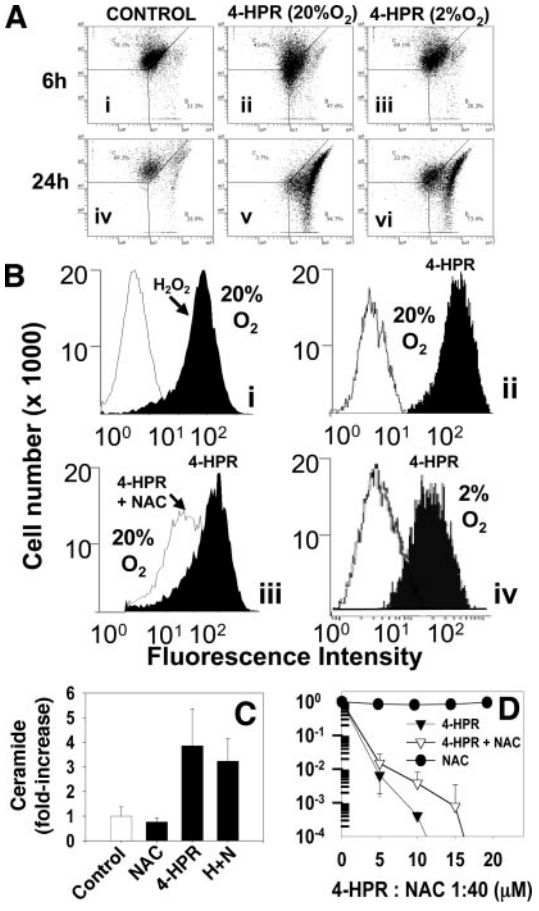

Fig. 4. Effects of hypoxia on *N*-(4-hydroxyphenyl) retinamide (4-HPR)-induced mitochondria membrane potential ($\Delta\Psi_m$) loss and effects of hypoxia and *N*-acetylcysteine (NAC) on 4-HPR-induced reactive oxygen species (ROS). *A*, 4-HPR-induced $\Delta\Psi_m$ loss in SK-N-MC cells treated with 4-HPR (10 μM) was determined using JC-1 dye (ratio of red to green fluorescence) in normoxia (20% O_2) for +6 h (*ii*) and +24 h (*v*) and in hypoxia (2% O_2) for +6 h (*iii*) and +24 h (*iv*). The ratio of red to green fluorescence was 3.6 (*i*), 0.9 (*ii*), and 2.4 (*iii*) at +6 h and 2.5 (*iv*), 0.03 (*v*), and 0.3 (*vi*) at +24 h, respectively. Hypoxia blunted 4-HPR-induced loss of $\Delta\Psi_m$ ($P < 0.05$). *B*, effect of 4-HPR (10 μM) on ROS in SK-N-MC cells treated with and without 1 mM NAC for 6 h in 20% O_2 and 2% O_2. ROS were analyzed by flow cytometry after addition of the redox-sensitive dye carboxy-DCFDA. *i*, increase of fluorescence in hydrogen peroxide (100 μM)-treated cells (positive controls, *filled histogram*) compared with untreated cells (*open histogram*). *ii*, in 20% O_2, 4-HPR increased ROS in SK-N-MC cells (*filled histogram*) compared with untreated cells (*open histogram*; $P = 0.03$). *iii*, NAC decreased the ROS generated by 4-HPR (*open histogram*) compared with 4-HPR-alone (*filled histogram*; $P = 0.01$). *iv*, in 2% O_2, ROS generation in SK-N-MC cells induced by 4-HPR (*filled histogram*) was decreased compared with treatment (*open histogram*) in 20% O_2 ($P = 0.04$). *C*, effect of NAC on 4-HPR-induced ceramide species in SK-N-MC cells. Preincubation with NAC (*H*+*N*) did not decrease 4-HPR-mediated ceramide species increase at +6 h ($P = 0.2$). *D*, effect of NAC on 4-HPR cytotoxicity in SK-N-MC cells. 4-HPR cytotoxicity in 20% O_2 was somewhat decreased ($P = 0.01$) at 4-HPR concentrations of ≥10 μM by addition of NAC (fixed 1:40 molar ratio of 4-HPR:NAC), although multilog cytotoxicity was retained.

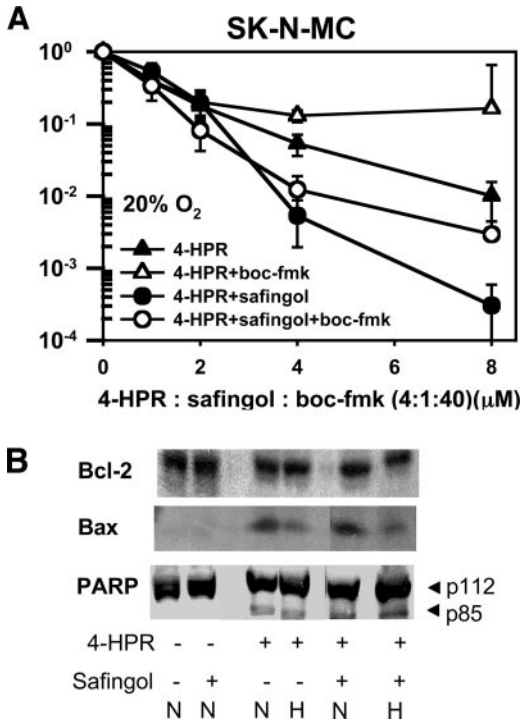

Fig. 5. Effects of pan-caspase inhibitor on *N*-(4-hydroxyphenyl) retinamide (4-HPR) cytotoxicity and of hypoxia on 4-HPR-induced bax expression. *A*, effect of pan-caspase inhibitor BOC-d-fmk on 4-HPR cytotoxicity. Dose response of SK-N-MC cells to 4-HPR (▲) and 4-HPR + safingol (4:1; ●) under normoxia at +96 h was assessed using the DIMSCAN assay. Preincubation (+8 h) with BOC-d-fmk (40 μM), followed by daily addition of BOC-d-fmk (40 μM), failed to abrogate 4-HPR (△) and 4-HPR + safingol (○) cytotoxicity. BOC-d-fmk treatment only increased the survival fraction from ~1% to ~15% for 4-HPR (8 μM) and from < 0.1% to ~1% for 4-HPR + safingol, indicating that cytotoxicity was substantially caspase independent. *Bars* indicate 95% confidence intervals. *B*, effect of hypoxia (2% O_2) on 4-HPR- and 4-HPR + safingol-induced bax and bcl-2 protein levels and poly(ADP-ribose) polymerase (PARP) cleavage. SK-N-MC cells were incubated with 4-HPR (10 μM) with or without safingol (2.5 μM) for +24 h. Cells were lysed, and immunoblotting was performed with anti-bcl-2, anti-bax, or anti-PARP antibody. 4-HPR induced a 6-fold increase in bax at +24 h (normalized to actin) in normoxia (*N, middle panel, Lane 3*). However, bax induction was decreased to 3-fold by hypoxia (*H, middle panel, Lane 4*). The combination of 4-HPR + safingol (4:1; *Lanes 5* and *6*) also induced bax expression (+5.9-fold at +24 h) in normoxia (*N*) and hypoxia (*H*; +2.9-fold at +24 h). PARP cleavage was induced at +24 h with 4-HPR alone or in combination with safingol (4:1; *bottom panel*). Bcl-2 expression remained unchanged by either treatment at +24 h (*top panel*).

ceramide species in SK-N-MC cells, lipid extracts were analyzed from SK-N-MC cells treated with 4-HPR (10 μM), with and without NOE (30 μM), in 20% O_2. 4-HPR + NOE increased ceramide species [up to 4-fold at +6 h ($P = 0.04$) and up to 13-fold at +24 h ($P = 0.1$); Fig. 6*D*], compared with 4-HPR alone (2-fold and 6-fold increases, respectively). Together, these data suggest that hypoxic induction of AC activity may decrease a portion of 4-HPR cytotoxicity that is dependent on increased ceramide species.

DISCUSSION

The mainstay of chemotherapy for ESFT is currently vincristine, cyclophosphamide, and doxorubicin, alternating with ifosfamide and etoposide (44). With these drugs and adequate local control of the primary tumor, many patients with localized ESFT (excepting those with pelvic primary tumors) can be cured. However, for patients with high-risk ESFT (which includes pelvic primary sites and metastatic disease at diagnosis), the prognosis is much worse, especially for tumors with spread to bone or bone marrow (3, 45). Attempts to improve outcome for high-risk ESFT using intensive induction therapy followed by myeloablative chemotherapy with stem cell rescue have achieved responses, but improvement in overall survival has been disappointing due to recurrent disease, especially in patients with bone and/or bone marrow metastases at diagnosis (3, 45–48).

One possible approach to improve therapy for metastatic ESFT could be to use intensive (myeloablative) chemoradiotherapy to maximally reduce tumor burden to a state of MRD and follow this with a maintenance therapy using drugs with modest systemic toxicity (especially to normal bone marrow). Ideally, such a maintenance therapy would have a biochemical mode of action that is different from that of the induction treatment to minimize the chances of cross-resistance. This approach was successfully used in treatment of high-risk neuroblastoma, in which a differentiating agent, 13-*cis*-retinoic acid, was used after myeloablative therapy (5). Unfortunately, unlike neuroblastoma (49), ESFT cell lines are not responsive to retinoic acid (50), and alternative agents must be identified.

The retinoid 4-HPR has cytotoxic antitumor activity against a variety of different solid tumor cell lines *in vitro* (4). The major

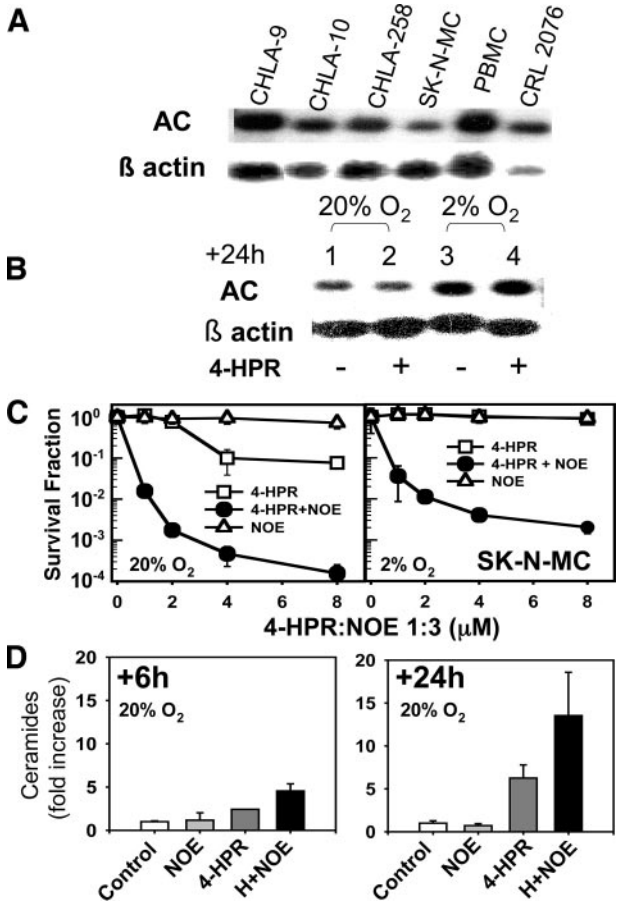

Fig. 6. Effect of hypoxia on acid ceramidase (AC) RNA levels in Ewing's sarcoma family of tumors cell lines and of AC inhibitor on ceramide species level and cytotoxicity. *A*, baseline AC expression in Ewing's sarcoma family of tumors cell lines, peripheral blood mononuclear cells (*PBMC*), and fibroblasts (*CRL 2076*) in 20% O_2 by Northern blot analysis. *B*, increase of AC RNA level in SK-N-MC cells by hypoxia (2% O_2), with (*Lanes 2* and *4*) and without (*Lanes 1* and *3*) *N*-(4-hydroxyphenyl) retinamide (4-HPR; 10 μM), at +24 h by Northern blot analysis. *C*, dose response of SK-N-MC cells in normoxia (20% O_2) and hypoxia (2% O_2) to 4-HPR (0–8 μM), with and without AC inhibitor *N*-oleoyl-ethanolamine (NOE; 1:3 molar ratio). NOE significantly increased 4-HPR cytotoxicity in both normoxia (*left panel*; combination index = 0.1) and hypoxia (*right panel*; combination index < 0.1; $P < 0.001$). *Bars* indicate 95% confidence intervals. *D*, effect of NOE on 4-HPR-induced ceramide species increase. In 20% O_2, SK-N-MC cells were exposed to 4-HPR (10 μM) with and without NOE (30 μM). 4-HPR increased labeled ceramide species 2.4 ± 0.1-fold ($P = 0.01$) and 6.2 ± 1.5-fold ($P = 0.006$) at +6 h and +24 h (*dark gray bars*), respectively, over control levels (*white bars*). Compared with 4-HPR alone, addition of NOE to 4-HPR further increased ceramide species level to 4.5 ± 0.8-fold ($P = 0.04$) and 13.5 ± 5.0-fold ($P = 0.1$) at +6 h and +24 h, respectively (*black bars*; note that ceramides species include dihydroceramides; see "Materials and Methods").

clinical toxicity of low-dose (1–3 μM) oral 4-HPR in adults is decreased night vision (51). In two recent pediatric oral 4-HPR Phase I trials, the average peak plasma concentration achieved was ~8–10 μM at the maximal tolerated dose of 2475 mg/m^2/day, divided into two or more doses a day (BID-TID; Ref. 12), and ~13 μM at the maximal practical dose of 4000 mg/m^2/day, given once daily, for 28 of 35 days, respectively (13), using a capsule formulation. Side effects included occasional hepatotoxicity and infrequent, non-dose-related pseudotumor cerebri, with no significant hematopoietic toxicity observed (12). The lack of hematopoietic toxicity makes 4-HPR an attractive agent to study in patients after myeloablative therapy or in multiply relapsed patients with decreased marrow function. We show here that 4-HPR has activity against ESFT cell lines *in vitro*, making it a candidate drug for treating ESFT in MRD. As we have observed previously in neuroblastoma (6, 14) and leukemia (15) cell lines, we have determined that 4-HPR increased ceramide species in ESFT cells *in vitro* by *de novo* synthesis. Our findings, together with evidence from other tumor types (14, 52–54), support a role for ceramide species in 4-HPR-induced tumor cell death.

Tumors are commonly hypoxic, and hypoxia has been shown to cause an up-regulation of prosurvival genes in cancer cells, confer a survival advantage to cancer cells, and antagonize common chemotherapeutic agents (55–58). Because we have shown previously that 4-HPR cytotoxicity for neuroblastoma cell lines is decreased by physiological hypoxia (6), we tested the effect of hypoxia on 4-HPR activity against ESFT cell lines. We chose an O_2 level of 2% for these studies because this is below the oxygen tension found in bone marrow (~4–5% O_2 equivalent tension), a site of metastatic ESFT disease. Additionally, 2% O_2 is representative of hypoxia found in solid tumor tissue (6, 56) and is in the range for hypoxia-increased activity of transcription factor hypoxia-inducible factor-1. Whereas the effect of hypoxia on 4-HPR cytotoxicity was variable in ESFT cell lines, overall, there was a decrease in 4-HPR cytotoxicity in 2% O_2 associated with a decrease in 4-HPR-induced ROS, $\Delta\psi_m$ loss, bax protein level, and ceramide species level, compared with 20% oxygen. These results suggest that 4-HPR delivered as a single agent may be more likely to demonstrate activity against ESFT disease in MRD settings in which oxygen tensions would be expected to be higher than in mass disease states.

Intracellular redox potential can play a significant role in commitment to apoptosis (59, 60). Our observations that, in hypoxia, 4-HPR caused a smaller change in $\Delta\Psi_m$, a lower level of ROS, and less increase of bax might partly explain the intermediate and downstream mechanisms of decreased 4-HPR cytotoxicity in hypoxia. Our data also indicate that the effect of hypoxia on 4-HPR-induced ceramide species in ESFT cells is independent of ROS because the thiol antioxidant NAC decreased the level of ROS (but not of ceramide species) induced by 4-HPR and only modestly decreased 4-HPR-induced cytotoxicity.

Seeking upstream mechanisms for hypoxia-induced reduction of ceramide species increase and 4-HPR cytotoxicity, we characterized the transcriptional response of SK-N-MC cells to hypoxia, with and without 4-HPR treatment, using oligonucleotide arrays. Among the ~400 genes (data not shown) with >2-fold changes of expression in hypoxia, we identified and validated the up-regulation of the AC gene. We demonstrated that 4-HPR cytotoxicity and 4-HPR-induced ceramide species increase were significantly enhanced by an AC inhibitor (NOE), even in hypoxia. Our results suggest that the decrease in cytotoxicity of 4-HPR in hypoxia in SK-N-MC cells may be partly due to up-regulation of AC and that characterizing other genes induced in hypoxia may provide additional potential targets for drugs to synergize 4-HPR cytotoxicity.

We have shown previously that safingol synergistically enhanced 4-HPR activity against cell lines from a variety of cancer cell types at drug levels minimally toxic to fibroblasts and marrow progenitors and that 4-HPR + safingol cytotoxicity is largely retained in hypoxia in neuroblastoma cell lines (14). Here we show that combining 4-HPR with safingol in a panel of ESFT cell lines caused a multilog, synergistic tumor cell kill, even in hypoxia, at levels of 4-HPR + safingol that are minimally toxic to hematopoietic progenitor cells (14). Moreover, the combination of 4-HPR and safingol was also highly effective against ESFT cell lines established at relapse that have nonfunctional p53. Clinically, safingol (at 120 mg/m^2) has been given as a 1-h infusion and achieved ~3 μM plasma levels without toxicity (61). These results suggest that the combination of 4-HPR + safingol may be tolerable clinically and demonstrate greater activity against ESFT disease in both MRD and mass disease than 4-HPR alone. Intravenous and improved oral formulations of 4-HPR and of i.v. safingol, to allow combination therapy, are currently under development with the support of National Cancer Institute Rapid Access to Intervention Development grants (to C. P. R. and B. J. M.).

The mechanism by which 4-HPR + safingol achieved such a striking and selective syngergistic cytotoxicity for tumor cells is not yet known, although we have reported that 4-HPR is not cytotoxic to and does not increase ceramide species in various nonmalignant cells (14, 15). Safingol has been reported to inhibit protein kinase C activity through inhibition of the phorbol regulatory subunit (62) and to inhibit sphingosine kinase activity (63, 64). Both these mechanisms could facilitate ceramide species-induced cytotoxicity. The significance of the latter inhibitory activity is not clear because it has mainly been assayed in platelets or cell extracts or using short-term (minutes) drug exposures (65–69). Furthermore, D,L-*threo*-dihydrosphinganine has been reported to be a substrate for human sphingosine kinase type 2 (70). Also, because protein kinase Cs may stimulate sphingosine kinase activity, distinguishing the primary effect(s) of *threo*-dihydrosphingosines in intact cells (primary sphingosine kinase inhibition *versus* secondary inhibition via protein kinase C inhibition) may be difficult (71, 72). Safingol, as a single agent in high doses (10 μM) induced apoptosis in a partially caspase-dependent manner (73). Our data suggest that the cytoxicity of 4-HPR and 4-HPR + safingol is only minimally dependent on caspase induction in EFST cell lines *in vitro*, although the possibility that the pan-caspase inhibitor used was not stable throughout the course of the cytoxicity assay cannot be excluded.

It is not clear whether safingol acts as a prodrug in whole cells. We and others have demonstrated that safingol is metabolized into L-*threo*-dihydroceramide and/or L-*threo*-ceramide variants, both *in vitro* (14, 74–77) and *in vivo* (78), with some disagreement between the data, perhaps due to species or cell line type variation. L-*threo*-dihydroceramide and/or L-*threo*-ceramide was incorporated into dihydrosphingomyelin or sphingomyelin but not readily glucosylated, thus demonstrating stereo-specific metabolic restrictions (14, 74, 75, 78). Because we and others have demonstrated that high levels of one or both of these L-*threo* sphingolipids accumulate even at low, nontoxic safingol concentrations *in vitro* (14), it is possible that L-*threo* sphingolipids may synergize the cytotoxicity of native *de novo*-generated ceramide species, including dihydroceramides (79, 80), by specific interference with their catabolism or may interfere with the ability of native ceramide species to activate atypical protein kinase Cs. Alternatively, these L-*threo* sphingolipids may represent cytotoxically inert metabolic products of safingol. If the latter is the case, then we speculate that safingol may be most effectively delivered clinically as a continuous infusion, rather than by bolus infusion, to maintain effective intracellular concentrations of the parent drug.

To further define the molecular mechanisms involved in the inhibition of 4-HPR cytotoxicity and the associated reduction of ceramide

species increase that occurs in ESFT under hypoxic conditions, we conducted gene expression analysis of the SK-N-MC cell line treated with 4-HPR in normoxic and hypoxic conditions. We observed an up-regulation of AC RNA levels (81) in hypoxia. The metabolic pathway for ceramides includes deacylation by alkaline, neutral, and AC (43, 82) to generate sphingosine, which can be phosphorylated by sphingosine kinase to form sphingosine-1-phosphate, a prosurvival molecule (83–86). Because ceramide degradation is the primary metabolic source of intracellular sphingosine, AC activity may be a determining step regulating intracellular levels of sphingosine, and subsequently sphingosine-1-phosphate, thereby playing an important role in cell survival (23). Although the intracellular access of AC activity to *de novo* ceramide species remains to be demonstrated, pharmacological inhibition of AC with NOE (43) at a 1:3 molar ratio (4-HPR:NOE) significantly increased levels of ceramide species and enhanced 4-HPR cytotoxicity. Whereas these results are suggestive, confirmation of AC involvement in hypoxia-related decrease in 4-HPR-induced cytotoxicity will require specific AC gene disruption studies.

In summary, 4-HPR is active against multiple ESFT cell lines in 20% O_2, but single-agent 4-HPR cytotoxicity and the associated increase of ceramide species are diminished by tumor-level hypoxia. The cytotoxicity of 4-HPR was synergistically enhanced by safingol in 20% O_2 and retained substantial activity in tumor-level hypoxia. These data support conducting further preclinical studies in ESFT, in support of clinical trials of 4-HPR, either as a single agent in the MRD setting (*i.e.*, in lesser degrees of hypoxia) or in combination with other agents (such as safingol) that may increase the cytotoxic properties of ceramide species (14).

ACKNOWLEDGMENTS

We thank Dr. Timothy J. Triche (Department of Pathology, Children's Hospital Los Angeles and Keck School of Medicine, University of Southern California) for assistance with oligonucleotide array analysis.

REFERENCES

1. Triche TJ, Askin FB. Neuroblastoma and the differential diagnosis of small-, round-, blue-cell tumors. Hum Pathol 1983;14:569–95.
2. Arvand A, Denny CT. Biology of EWS/ETS fusions in Ewing's family tumors. Oncogene 2001;20:5747–54.
3. Kushner BH, Meyers PA. How effective is dose-intensive/myeloablative therapy against Ewing's sarcoma/primitive neuroectodermal tumor metastatic to bone or bone marrow? The Memorial Sloan-Kettering experience and a literature review. J Clin Oncol 2001;19:870–80.
4. Reynolds CP, Lemons RS. Retinoid therapy of childhood cancer. Hematol Oncol Clin North Am 2001;15:867–910.
5. Matthay KK, Villablanca JG, Seeger RC, et al. Treatment of high-risk neuroblastoma with intensive chemotherapy, radiotherapy, autologous bone marrow transplantation, and 13-cis-retinoic acid. Children's Cancer Group. N Engl J Med 1999;341:1165–73.
6. Maurer BJ, Metelitsa LS, Seeger RC, Cabot MC, Reynolds CP. Increase of ceramide and induction of mixed apoptosis/necrosis by N-(4-hydroxyphenyl)-retinamide in neuroblastoma cell lines. J Natl Cancer Inst (Bethesda) 1999;91:1138–46.
7. Delia D, Aiello A, Meroni L, et al. Role of antioxidants and intracellular free radicals in retinamide-induced cell death. Carcinogenesis (Lond) 1997;18:943–8.
8. Oridate N, Suzuki S, Higuchi M, et al. Involvement of reactive oxygen species in N-(4-hydroxyphenyl)retinamide-induced apoptosis in cervical carcinoma cells. J Natl Cancer Inst (Bethesda) 1997;89:1191–8.
9. Sun SY, Yue P, Lotan R. Induction of apoptosis by N-(4-hydroxyphenyl)retinamide and its association with reactive oxygen species, nuclear retinoic acid receptors, and apoptosis-related genes in human prostate carcinoma cells. Mol Pharmacol 1999;55:403–10.
10. Wu JM, DiPietrantonio AM, Hsieh TC. Mechanism of fenretinide (4-HPR)-induced cell death. Apoptosis 2001;6:377–88.
11. Costa A, Formelli F, Chiesa F, et al. Prospects of chemoprevention of human cancers with the synthetic retinoid fenretinide. Cancer Res 1994;54:2032s–7s.
12. Villablanca JG, Ames MM, Reid JM, et al. Phase I trial of oral N-(-4-hydroxyphenyl)retinamide (4-HPR) in children with resistant/recurrent solid tumors: a Children's Cancer Group study (CCG 09709). Proc Am Soc Clin Oncol 2002;21:398a.
13. Garaventa A, Luksch R, Piccolo MS, et al. Phase I trial and pharmacokinetics of fenretinide in children with neuroblastoma. Clin Cancer Res 2003;9:2032–9.
14. Maurer BJ, Melton L, Billups C, Cabot MC, Reynolds CP. Synergistic cytotoxicity in solid tumor cell lines between N-(4-hydroxyphenyl)retinamide and modulators of ceramide metabolism. J Natl Cancer Inst (Bethesda) 2000;92:1897–909.
15. O'Donnell PH, Guo WX, Reynolds CP, Maurer BJ. N-(4-hydroxyphenyl)retinamide increases ceramide and is cytotoxic to acute lymphoblastic leukemia cell lines, but not to non-malignant lymphocytes. Leukemia (Baltimore) 2002;16:902–10.
16. Reynolds CP, Maurer BJ, Kolesnick R. Ceramide synthesis and metabolism as a target for cancer therapy. Cancer Lett 2004;206:169–80.
17. Kolesnick RN, Goni FM, Alonso A. Compartmentalization of ceramide signaling: physical foundations and biological effects. J Cell Physiol 2000;184:285–300.
18. Ruvolo PP. Ceramide regulates cellular homeostasis via diverse stress signaling pathways. Leukemia (Baltimore) 2001;15:1153–60.
19. Basu S, Kolesnick R. Stress signals for apoptosis: ceramide and c-Jun kinase. Oncogene 1998;17:3277–85.
20. Liu YY, Han TY, Giuliano AE, Cabot MC. Expression of glucosylceramide synthase, converting ceramide to glucosylceramide, confers Adriamycin resistance in human breast cancer cells. J Biol Chem 1999;274:1140–6.
21. Abe A, Shayman JA, Radin NS. A novel enzyme that catalyzes the esterification of N-acetylsphingosine. Metabolism of C2-ceramides. J Biol Chem 1996;271:14383–9.
22. Hiraoka M, Abe A, Shayman JA. Cloning and characterization of a lysosomal phospholipase A2, 1-O-acylceramide synthase. J Biol Chem 2002;277:10090–9.
23. Strelow A, Bernardo K, Adam-Klages S, et al. Overexpression of acid ceramidase protects from tumor necrosis factor-induced cell death. J Exp Med 2000;192:601–12.
24. Biedler JL, Spengler BA. A novel chromosome abnormality in human neuroblastoma and antifolate-resistant Chinese hamster cell lives in culture. J Natl Cancer Inst (Bethesda) 1976;57:683–95.
25. Schlesinger HR, Gerson JM, Moorhead PS, Maguire H, Hummeler K. Establishment and characterization of human neuroblastoma cell lines. Cancer Res 1976;36:3094–100.
26. Whang-Peng J, Triche TJ, Knutsen T, et al. Chromosome translocation in peripheral neuroepithelioma. N Engl J Med 1984;311:584–5.
27. Fragala T, Proffitt RT, Reynolds CP. A novel 96-well plate cytotoxicity assay based on fluorescence digital imaging microscopy. Proc Am Assoc Cancer Res 1995;36:303.
28. Proffitt RT, Tran JV, Reynolds CP. A fluorescence digital image microscopy system for quantifying relative cell numbers in tissue culture plates. Cytometry 1996;24:204–13.
29. Keshelava N, Seeger RC, Groshen S, Reynolds CP. Drug resistance patterns of human neuroblastoma cell lines derived from patients at different phases of therapy. Cancer Res 1998;58:5396–405.
30. Lavie Y, Cao H, Bursten SL, Giuliano AE, Cabot MC. Accumulation of glucosylceramides in multidrug-resistant cancer cells. J Biol Chem 1996;271:19530–6.
31. Merrill AH Jr, Wang E, Gilchrist DG, Riley RT. Fumonisins and other inhibitors of de novo sphingolipid biosynthesis. Adv Lipid Res 1993;26:215–34.
32. Darzynkiewicz Z, Bruno S, Del Bino G, et al. Features of apoptotic cells measured by flow cytometry. Cytometry 1992;13:795–808.
33. Yang B, Keshelava N, Anderson CP, Reynolds CP. Antagonism of buthionine sulfoximine cytotoxicity for human neuroblastoma cell lines by hypoxia is reversed by the bioreductive agent tirapazamine. Cancer Res 2003;63:1520–6.
34. Keshelava N, Zuo JJ, Chen P, et al. Loss of p53 function confers high-level multidrug resistance in neuroblastoma cell lines. Cancer Res 2001;61:6185–93.
35. Wang Y, Einhorn P, Triche TJ, Seeger RC, Reynolds CP. Expression of protein gene product 9.5 and tyrosine hydroxylase in childhood small round cell tumors. Clin Cancer Res 2000;6:551–8.
36. Lockhart DJ, Dong H, Byrne MC, et al. Expression monitoring by hybridization to high-density oligonucleotide arrays. Nat Biotechnol 1996;14:1675–80.
37. Chou TC, Hayball MP. Calcusyn manual: Windows Software for dose effect analysis. Cambridge, United Kingdom: Biosoft; 1996.
38. Chou TC. Drug combinations: from laboratory to practice. J Lab Clin Med 1998;132:6–8.
39. Batra S, Wedgeworth EK, Triche TJ, Wu S, Reynolds CP. Progressive increase in resistance to cytotoxic drugs in cell lines from primitive neuroectodermal tumors established at diagnosis, after chemotherapy, and after myeloablative chemotherapy. Proc Am Assoc Cancer Res 2003;44:1151.
40. Lovat PE, Ranalli M, Annichiarrico-Petruzzelli M, et al. Effector mechanisms of fenretinide-induced apoptosis in neuroblastoma. Exp Cell Res 2000;260:50–60.
41. Shen JC, Wang TT, Chang S, Hursting SD. Mechanistic studies of the effects of the retinoid N-(4-hydroxyphenyl)retinamide on prostate cancer cell growth and apoptosis. Mol Carcinog 1999;24:160–8.
42. Sugita M, Willians M, Dulaney JT, Moser HW. Ceramidase and ceramide synthesis in human kidney and cerebellum. Description of a new alkaline ceramidase. Biochim Biophys Acta 1975;398:125–31.
43. Raisova M, Goltz G, Bektas M, et al. Bcl-2 overexpression prevents apoptosis induced by ceramidase inhibitors in malignant melanoma and HaCaT keratinocytes. FEBS Lett 2002;516:47–52.
44. Meyers PA, Levy AS. Ewing's sarcoma. Curr Treat Options Oncol 2000;1:247–57.
45. Burdach S, Jurgens H. High-dose chemoradiotherapy (HDC) in the Ewing family of tumors (EFT). Crit Rev Oncol Hematol 2002;41:169–89.
46. Madero L, Munoz A, Sanchez DT, et al. Megatherapy in children with high-risk Ewing's sarcoma in first complete remission. Bone Marrow Transplant 1998;21:795–9.
47. Bader JL, Horowitz ME, Dewan R, et al. Intensive combined modality therapy of small round cell and undifferentiated sarcomas in children and young adults: local control and patterns of failure. Radiother Oncol 1989;16:189–201.

48. Miser JS, Kinsella TJ, Triche TJ, et al. Preliminary results of treatment of Ewing's sarcoma of bone in children and young adults: six months of intensive combined modality therapy without maintenance. J Clin Oncol 1988;6:484–90.
49. Reynolds CP, Matthay KK, Villablanca JG, Maurer BJ. Retinoid therapy of high-risk neuroblastoma. Cancer Lett 2003;197:185–92.
50. Cavazzana AO, Miser JS, Jefferson J, Triche TJ. Experimental evidence for a neural origin of Ewing's sarcoma of bone. Am J Pathol 1987;127:507–18.
51. Torrisi R, Parodi S, Fontana V, et al. Factors affecting plasma retinol decline during long-term administration of the synthetic retinoid fenretinide in breast cancer patients. Cancer Epidemiol Biomark Prev 1994;3:507–10.
52. DiPietrantonio AM, Hsieh TC, Olson SC, Wu JM. Regulation of G1/S transition and induction of apoptosis in HL-60 leukemia cells by fenretinide (4HPR). Int J Cancer 1998;78:53–61.
53. Senchenkov A, Litvak DA, Cabot MC. Targeting ceramide metabolism: a strategy for overcoming drug resistance. J Natl Cancer Inst (Bethesda) 2001;93:347–57.
54. Prinetti A, Basso L, Appierto V, et al. Altered sphingolipid metabolism in N-(4-hydroxyphenyl)-retinamide-resistant A2780 human ovarian carcinoma cells. J Biol Chem 2003;278:5574–83.
55. Brown JM. The hypoxic cell: a target for selective cancer therapy–eighteenth Bruce F. Cain Memorial Award lecture. Cancer Res 1999;59:5863–70.
56. Moulder JE, Rockwell S. Tumor hypoxia: its impact on cancer therapy. Cancer Metastasis Rev 1987;5:313–41.
57. Brown JM, Koong A. Therapeutic advantage of hypoxic cells in tumors: a theoretical study. J Natl Cancer Inst (Bethesda) 1991;83:178–85.
58. Workman P, Stratford IJ. The experimental development of bioreductive drugs and their role in cancer therapy. Cancer Metastasis Rev 1993;12:73–82.
59. Zamzami N, Marchetti P, Castedo M, et al. Sequential reduction of mitochondrial transmembrane potential and generation of reactive oxygen species in early programmed cell death. J Exp Med 1995;182:367–77.
60. Joza N, Susin SA, Daugas E, et al. Essential role of the mitochondrial apoptosis-inducing factor in programmed cell death. Nature (Lond) 2001;410:549–54.
61. Schwartz GK, Ward D, Saltz L, et al. A pilot clinical/pharmacological study of the protein kinase C-specific inhibitor safingol alone and in combination with doxorubicin. Clin Cancer Res 1997;3:537–43.
62. Wilson E, Olcott MC, Bell RM, Merrill AH Jr, Lambeth JD. Inhibition of the oxidative burst in human neutrophils by sphingoid long-chain bases. Role of protein kinase C in activation of the burst. J Biol Chem 1986;261:12616–23.
63. Chao CP, Laulederkind SJ, Ballou LR. Sphingosine-mediated phosphatidylinositol metabolism and calcium mobilization. J Biol Chem 1994;269:5849–56.
64. Choi OH, Kim JH, Kinet JP. Calcium mobilization via sphingosine kinase in signalling by the Fc epsilon RI antigen receptor. Nature (Lond) 1996;380:634–6.
65. Buehrer BM, Bell RM. Inhibition of sphingosine kinase in vitro and in platelets. Implications for signal transduction pathways. J Biol Chem 1992;267:3154–9.
66. Edsall LC, Van Brocklyn JR, Cuvillier O, Kleuser B, Spiegel SN. N-Dimethylsphingosine is a potent competitive inhibitor of sphingosine kinase but not of protein kinase C: modulation of cellular levels of sphingosine 1-phosphate and ceramide. Biochemistry 1998;37:12892–8.
67. Banno Y, Kato M, Hara A, Nozawa Y. Evidence for the presence of multiple forms of Sph kinase in human platelets. Biochem J 1998;335:301–4.
68. Blaukat A, Dikic I. Activation of sphingosine kinase by the bradykinin B2 receptor and its implication in regulation of the ERK/MAP kinase pathway. Biol Chem 2001;382:135–9.
69. Yang L, Yatomi Y, Satoh K, Igarashi Y, Ozaki Y. Sphingosine 1-phosphate formation and intracellular Ca^{2+} mobilization in human platelets: evaluation with sphingosine kinase inhibitors. J Biochem (Tokyo) 1999;126:84–9.
70. Liu H, Sugiura M, Nava VE, et al. Molecular cloning and functional characterization of a novel mammalian sphingosine kinase type 2 isoform. J Biol Chem 2002;275:19513–20.
71. Tolan D, Conway AM, Rakhit S, Pyne N, Pyne S. Assessment of the extracellular and intracellular actions of sphingosine 1-phosphate by using the p42/p44 mitogen-activated protein kinase cascade as a model. Cell Signal 1999;11:349–54.
72. Buehrer BM, Bardes ES, Bell RM. Protein kinase C-dependent regulation of human erythroleukemia (HEL) cell sphingosine kinase activity. Biochim Biophys Acta 1996;1303:233–42.
73. Amin HM, Ergin M, Denning MF, Quevedo ME, Alkan S. Characterization of apoptosis induced by protein kinase C inhibitors and its modulation by the caspase pathway in acute promyelocytic leukaemia. Br J Haematol 2000;110:552–62.
74. Venkataraman K, Futerman AH. Comparison of the metabolism of L-erythro- and L-threo-sphinganines and ceramides in cultured cells and in subcellular fractions. Biochim Biophys Acta 2001;1530:219–26.
75. Dragusin M, Gurgui C, Schwarzmann G, Hoernschemeyer J, Echten-Deckert G. Metabolism of the unnatural anticancer lipid safingol, L-threo-dihydrosphingosine, in cultured cells. J Lipid Res 2003;44:1772–9.
76. Humpf HU, Schmelz EM, Meredith FI, et al. Acylation of naturally occurring and synthetic 1-deoxysphinganines by ceramide synthase. Formation of N-palmitoyl-aminopentol produces a toxic metabolite of hydrolyzed fumonisin, AP1, and a new category of ceramide synthase inhibitor J Biol Chem 1998;273:19060–4.
77. Michel C, Echten-Deckert G, Rother J, et al. Characterization of ceramide synthesis. A dihydroceramide desaturase introduces the 4,5-trans-double bond of sphingosine at the level of dihydroceramide J Biol Chem 1997;272:22432–7.
78. Stoffel W, Bister K. Stereospecificities in the metabolic reactions of the four isomeric sphinganines (dihydrosphingosines) in rat liver. Hoppe-Seyler's Z Physiol Chem 1973;354:169–81.
79. Shikata K, Niiro H, Azuma H, Ogino K, Tachibana T. Apoptotic activities of C2-ceramide and C2-dihydroceramide homologues against HL-60 cells. Bioorg Med Chem 2003;11:2723–8.
80. Kok JW, Nikolova-Karakashian M, Klappe K, Alexander C, Merrill AH Jr. Dihydroceramide biology. Structure-specific metabolism and intracellular localization J Biol Chem 1997;272:21128–36.
81. Ferlinz K, Kopal G, Bernardo K, et al. Human acid ceramidase: processing, glycosylation, and lysosomal targeting. J Biol Chem 2001;276:35352–60.
82. Li CM, Park JH, He X, et al. The human acid ceramidase gene (ASAH): structure, chromosomal location, mutation analysis, and expression. Genomics 1999;62:223–31.
83. Cuvillier O, Rosenthal DS, Smulson ME, Spiegel S. Sphingosine 1-phosphate inhibits activation of caspases that cleave poly(ADP-ribose) polymerase and lamins during Fas- and ceramide-mediated apoptosis in Jurkat T lymphocytes. J Biol Chem 1998;273:2910–6.
84. Spiegel S, Cuvillier O, Edsall L, et al. Roles of sphingosine-1-phosphate in cell growth, differentiation, and death. Biochemistry (Mosc) 1998;63:69–73.
85. Olivera A, Kohama T, Edsall L, et al. Sphingosine kinase expression increases intracellular sphingosine-1-phosphate and promotes cell growth and survival. J Cell Biol 1999;147:545–58.
86. Cuvillier O, Pirianov G, Kleuser B, et al. Suppression of ceramide-mediated programmed cell death by sphingosine-1-phosphate. Nature (Lond) 1996;381:800–3.